Engine Yaw Augmentation for Hybrid-Wing-Body Aircraft via Optimal Control Allocation Techniques

Brian R. Taylor[1] and Seung Y. Yoo[2]
NASA Dryden Flight Research Center, Edwards, California, 93523

Asymmetric engine thrust was implemented in a hybrid-wing-body non-linear simulation to reduce the amount of aerodynamic surface deflection required for yaw stability and control. Hybrid-wing-body aircraft are especially susceptible to yaw surface deflection due to their decreased bare airframe yaw stability resulting from the lack of a large vertical tail aft of the center of gravity. Reduced surface deflection, especially for trim during cruise flight, could reduce the fuel consumption of future aircraft. Designed as an add-on, optimal control allocation techniques were used to create a control law that tracks total thrust and yaw moment commands with an emphasis on not degrading the baseline system. Implementation of engine yaw augmentation is shown and feasibility is demonstrated in simulation with a potential drag reduction of 2 to 4 percent. Future flight tests are planned to demonstrate feasibility in a flight environment.

Nomenclature

B	=	engine moment arm
HWB	=	hybrid-wing-body
J	=	cost
NASA	=	National Aeronautics and Space Administration
PLA	=	power lever angle
T	=	individual delta desired thrust
u	=	individual delta engine thrust
v	=	aero-achieved yaw moment
ε	=	second objective weighting matrix
γ	=	third objective weighting matrix

I. Introduction

Reduced environmental impact of future aircraft is both a national and a National Aeronautics and Space Administration (NASA) goal.[1] Hybrid-wing-body (HWB) aircraft have been identified as a potential aircraft configuration to meet this goal through an aerodynamically efficient shape that also reduces engine noise. One challenge associated with HWB aircraft is reduced bare airframe yaw stability and control authority due to the lack of a large vertical tail with a large moment arm aft of the center of gravity. Some HWB aircraft, such as the X-48B unmanned aerial vehicle (The Boeing Company, Chicago, Illinois), augment the bare airframe yaw stability and control with a closed-loop flight control system that uses split ailerons at the wingtips to create yaw moment with asymmetric drag.[2] This approach has the disadvantage of creating drag and reducing the aerodynamic efficiency benefits of the HWB configuration. This paper presents a solution that uses asymmetric engine thrust to create yaw moments for trim or relatively slow maneuvers.

Propulsion-controlled aircraft research for civilian transport applications began in earnest following the complete loss of hydraulic power on United Airlines Flight 232.[3] Upon loss of conventional flight controls, the pilots of that flight manually operated the engines in order to control the aircraft and attempted a landing in Sioux City, Iowa. While not completely successful, the pilots' efforts have been credited with saving many lives. This mishap and the pilots' actions led to extensive research in the use of propulsion control to replace or augment the control authority of the baseline aircraft in the event of failures.[4-15] Additional applications of such thrust vectoring have included

[1] Aerospace Engineer, Controls and Dynamics Branch, P.O. Box 273, MS 4840D, AIAA Member.
[2] Aerospace Engineer, Controls and Dynamics Branch, P.O. Box 273, MS 4840D, AIAA Member.

research on a NASA F-15 airplane (McDonnell Douglas, now The Boeing Company, Chicago, Illinois) to investigate trim drag reductions resulting in a 3.5-percent drag reduction for pitch thrust vectoring and a 1.5-percent drag reduction for yaw thrust vectoring.[16]

The controller presented in this paper is unique in that it is intended to reduce surface activity during trim and low-frequency yaw inputs for HWB aircraft. The controller was designed as an extension to the baseline control laws to reduce the verification and validation required. High-frequency stability and control is preserved, and low-frequency augmentation is handled by an optimal control allocator with thrust command and yaw tracking.

II. Aircraft Description

The aircraft used for this simulation study and planned flight research is the X-48B unmanned aerial vehicle, shown in Fig. 1. The X-48B is a joint partnership between NASA, the Air Force Research Laboratory (AFRL), and The Boeing Company. Built by Cranfield Aerospace Limited (United Kingdom), the aircraft is an 8.5-percent dynamically scaled HWB with 20 aerodynamic control surfaces and three JetCat (JetCat USA, Paso Robles, California) turbojet engines.

Figure 1. The X-48B aircraft in flight.

The X-48B aircraft can be configured with varying ground-adjustable slat and center of gravity configurations; however, only one configuration was used for this study. The baseline X-48B control system runs at 200 Hz[17] and uses a nonlinear dynamic inversion with a pseudo-daisy-chain control allocation. The baseline control allocation prior to surface saturation is depicted in Fig. 2; surfaces and engines are numbered for reference. Surface 6 and surface 7 are split ailerons: the top and bottom surface can be moved together to produce roll moments or they can be split to create asymmetric drag and produce a yaw moment. Rudders are also incorporated into the winglets to provide yaw control.

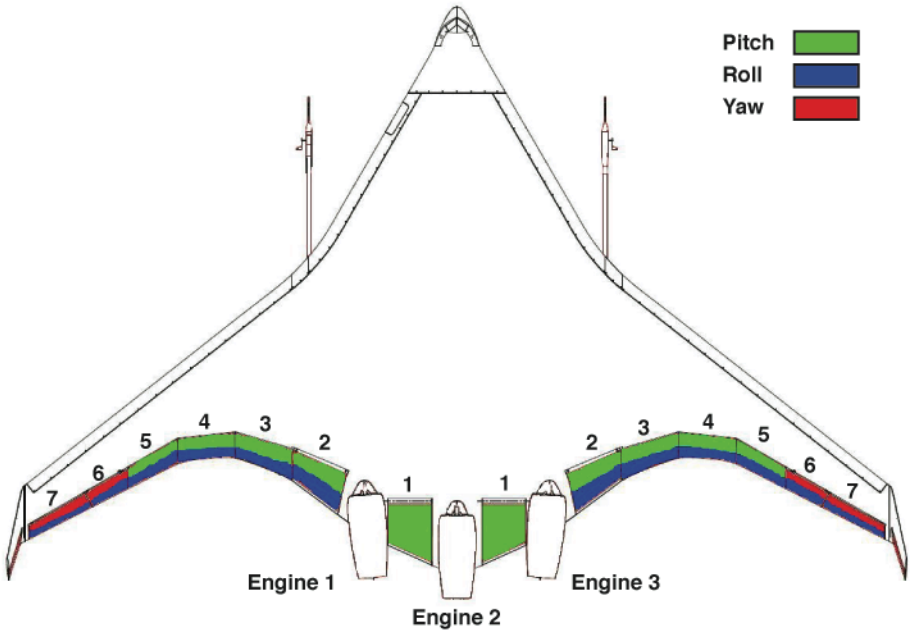

Figure 2. The control surface allocation of the X-48B aircraft.

III. Engine Yaw Control

In general, the goals of the engine yaw add-on were to preserve the baseline aircraft control characteristics and to reduce the amount of control surface deflection. A block diagram for the add-on controller is shown in Fig. 3. The controller was implemented in the X-48B control laws by intercepting and adjusting the revolutions per minute (rpm) commands just prior to being sent to the engine control units. The baseline control laws had no knowledge of the engine add-on. Low-pass filters with a cutoff frequency of 0.5 rad/s were put on all of the control inputs to add robustness against noise for planned flight-testing.

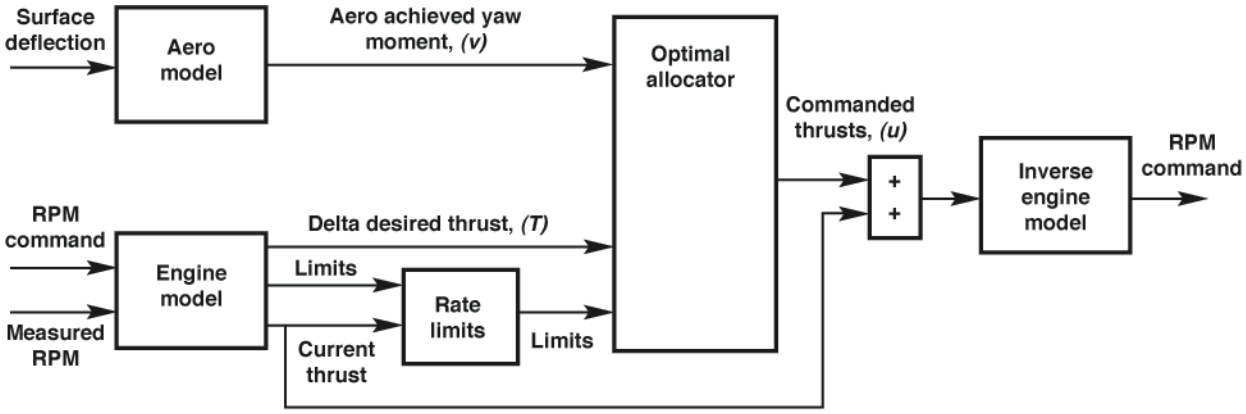

Figure 3. Block diagram of the engine yaw augmentation.

Optimal allocation techniques were used to determine the optimal thrust for each engine in order to meet the objectives. More information about optimal control allocation can be found in Ref. 18. The allocation objectives, in priority order, were: to track the total thrust command from the power lever angle (PLA), to generate yaw moment in order to drive the split ailerons to zero, and to keep the individual engines as close to their individual PLA commands as possible. Total thrust tracking and yaw moment objectives were used to maintain the baseline handling of the aircraft and reduce control surface deflections. Individual PLA tracking was added to reduce the

engine response time and reduce the severity of transients if the engine yaw add-one were switched off suddenly. This objective also reduces the amount of rpm changes commanded to each engine, which should prolong engine life. Equation 1 is the cost function to be minimized in order to meet these objectives. This equation was implemented in the "optimal allocator" block in Fig. 3.

Total Thrust Yaw Moment Individual PLA

$$J = \left|\sum_{i=1}^{3}\left(T_i - u_i\right)\right| + \varepsilon|v - Bu| + \gamma\sqrt{\left(T_1 - u_1\right)^2 + \left(T_2 - u_2\right)^2 + \left(T_3 - u_3\right)^2} \quad (1)$$

Find the minimum of

subject to: $u_{i_{\min}} \le u_i \le u_{i_{\max}}$

where T is a vector of individual delta desired thrust, which was defined as the individual difference between commanded and current thrust. Commanded thrust was computed with the individual PLA and an engine model, while current thrust was estimated with measured rpm and an engine model. The value v is the aero-achieved yaw moment estimated by the split-aileron deflection multiplied by its control effectiveness. Only the split-aileron deflections were used because they contribute more to the aircraft drag than do the winglet rudders. The vector B is the moment arm of the engines, and ε, γ are weighting matrices to weight the objectives according to their priority. The value u is a vector of the individual optimal delta engine thrusts from the optimal allocator and was added to the current thrust for a total thrust command. These total commands were then passed through an inverse engine model to transform them back to rpm commands to be sent to the engines.

Current thrust was used to rate limit the allocator. Due to the slow nature of the engines and the relative imprecision with which they can be commanded, the rate limiting allowed for a smaller solution space to be used. The entire solution space was searched rather than employing a gradient search method. Cost was computed for every possible combination of commanded engine thrust. The combination with the minimum cost, the optimal allocation, was selected. The solution space was +/-3 percent of the total engine thrust with a step size of 1 percent of the total engine thrust, resulting in 343 computations per frame.

The engine add-on acts as a perturbation controller to the baseline system. The baseline system responds to disturbances or yaw commands with aerodynamic surfaces. After deflection of the split ailerons is measured, the engine add-on commands asymmetric thrust. The baseline system then responds to this asymmetric thrust by reducing the amount of split-aileron deflection in order to maintain the desired aircraft state. This cycle continues until the split ailerons are driven to zero or the engine add-on runs out of authority. There is some inherent delay between the disturbance and the use of asymmetric engine thrust due to using sensed surface position. In addition, the engines themselves act as a low-pass filter.

IV. Simulation Results

The add-on engine yaw controller was integrated with the X-48B baseline control laws in a non-linear simulation. Three objectives were to: ensure the engine yaw controller did not degrade the performance of the baseline control laws, measure the benefits of the engine yaw controller, and ensure the engine yaw controller is robust to instrumentation and modeling errors.

First, lateral-directional frequency response was tested to ensure that the engine yaw control did not degrade the baseline control laws. Frequency sweeps of the engine model indicated that 6 dB attenuation occurred at a frequency of 1 Hz, so the engine yaw controller should have no effect on the baseline control laws above that frequency. Frequency sweeps for rudder-to-sideslip angle were tested in simulation with the engine yaw add-on turned on and off (see Fig. 4). As expected, the frequency response remained in phase with small variations in magnitude; it was concluded that the engine yaw add-on did not harm the low-frequency stability and control of the aircraft.

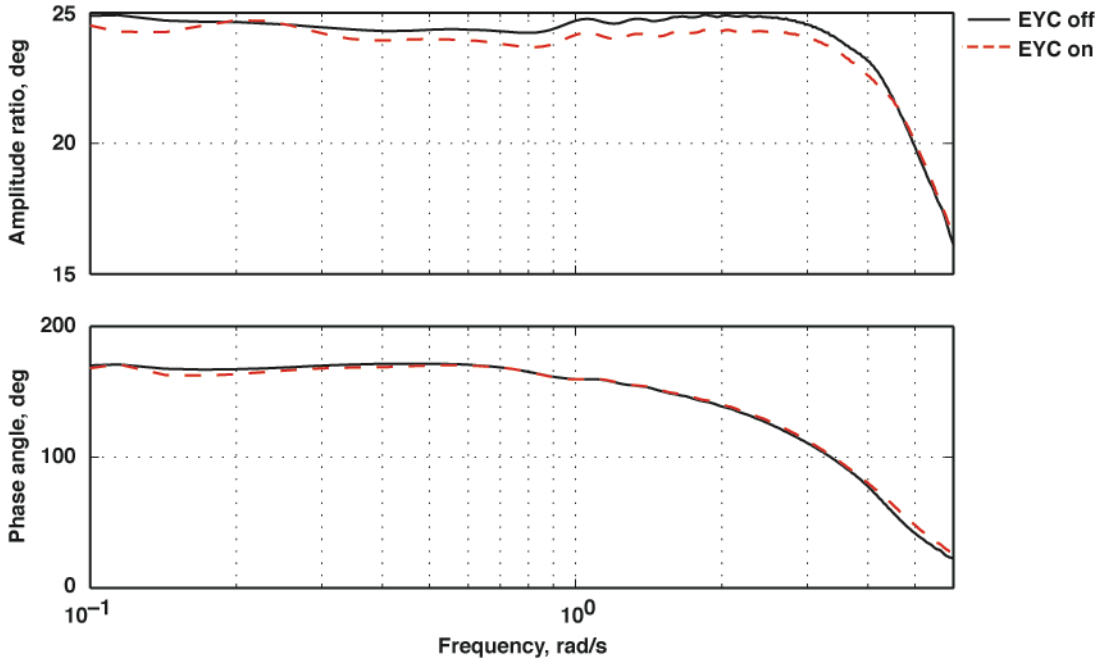

Figure 4. Engine yaw frequency response.

Next, performance of the engine yaw controller at a range of PLA settings was tested in simulation to ensure that the aerodynamic yaw surfaces are driven to zero while always tracking the total thrust commands. The maneuver used to check this was a rudder step followed by a PLA ramp, as shown in Figs. 5a through 5d. The rudder step was 2 percent of the maximum sideslip angle; it was input at 2 s and held for the remaining duration. The PLA ramp was approximately a linear ramp input at 80 s, shown by the total thrust command in Figs. 5a and 5d.

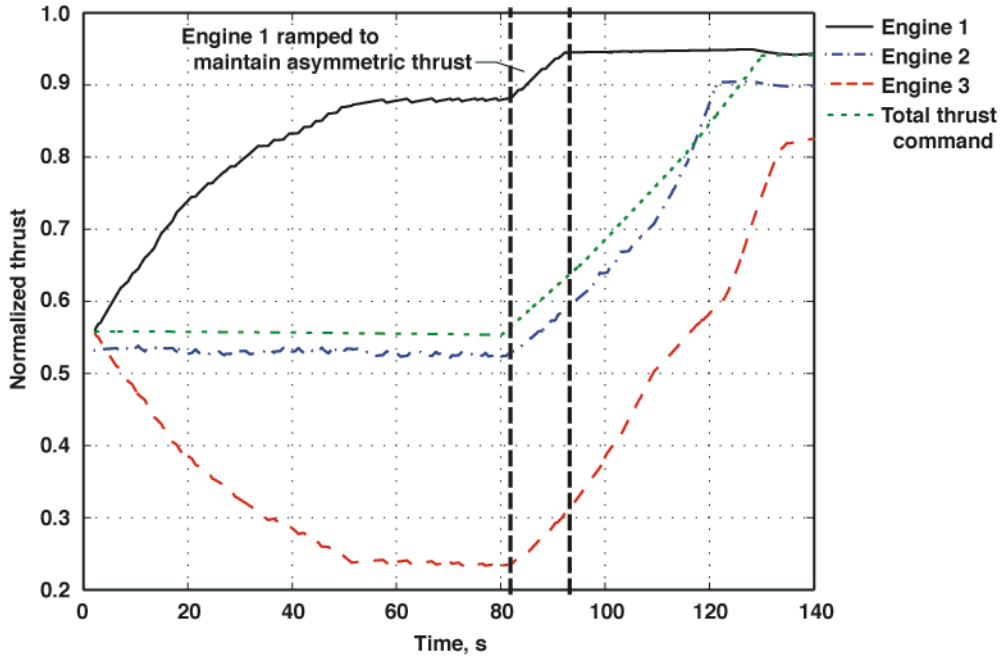

Figure 5a. Individual thrust response, rudder step, and power lever angle ramp.

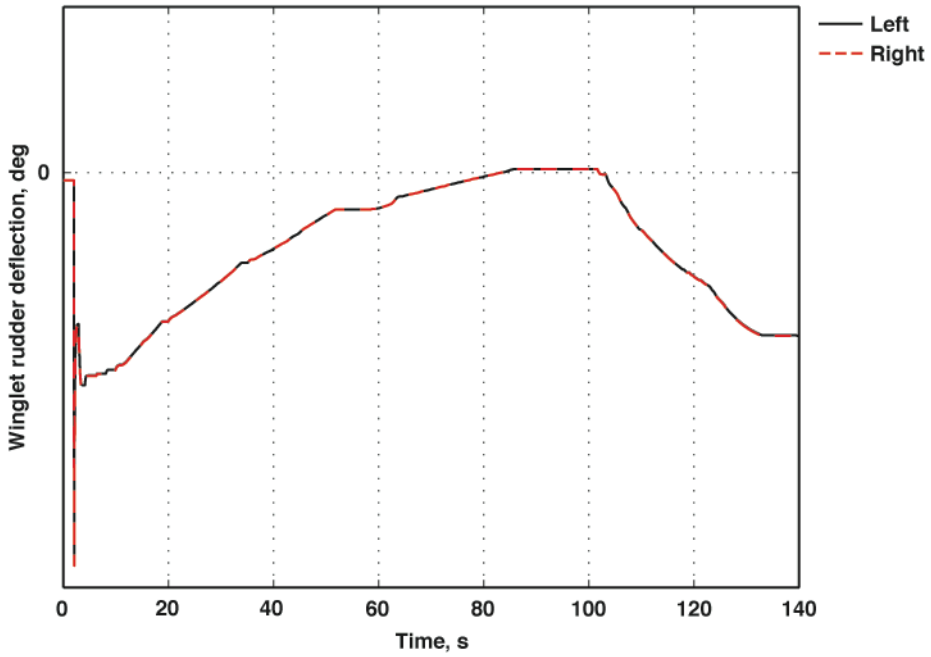

Figure 5b. Winglet rudder response, rudder step, and power lever angle ramp.

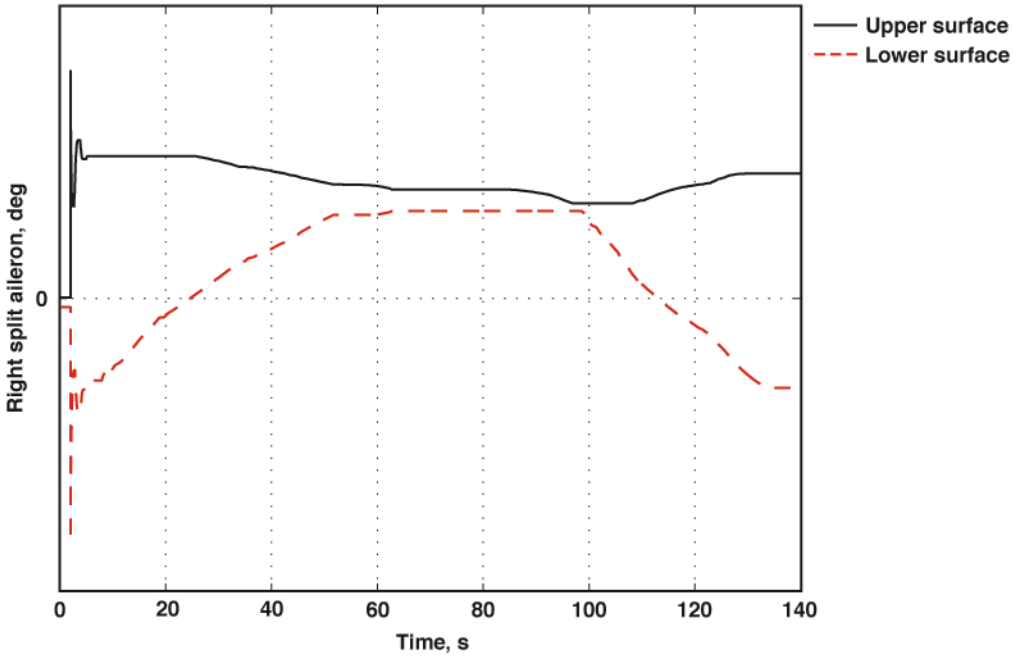

Figure 5c. Right split aileron response, rudder step, and power lever angle response.

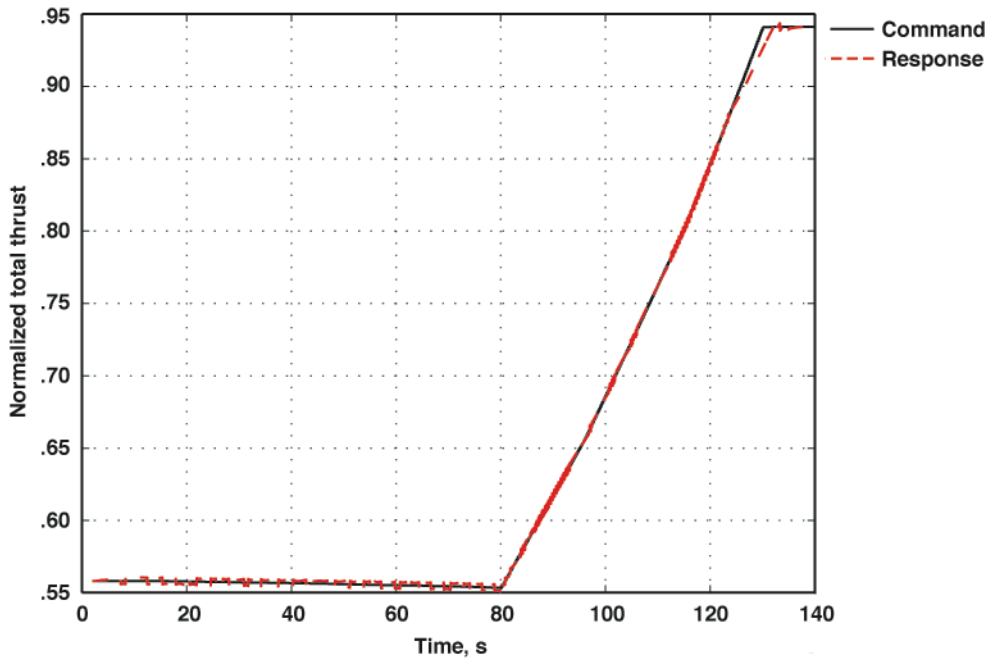

Figure 5d. Total thrust response, rudder step, and power lever angle ramp.

Initially, the thrust from engines 1 and 3 is split to produce a yawing moment, shown in Fig. 5a. This yawing moment is sufficient to drive the split ailerons and winglet rudders to zero with a convergence time of approximately 50 s, as shown in Figs. 5b and 5c. Convergence time is primarily dictated by the limits set in the "Rate Limits" block shown in Fig. 2 and the weighting factor used on the yaw moment portion of the cost function in Eq. (1). As the PLA is ramped up starting at 80 s, thrust on all of the engines is increased to meet the total thrust command and the aerodynamic surfaces are used to meet most of the commanded yaw moment. Notice from Fig. 5a from approximately 82 s to 92 s, thrust on engine 1 is increased to maintain yawing moment. At approximately 92 s, engine 1 reaches its maximum thrust and is no longer able to maintain the same level of asymmetric thrust as before. Aerodynamic surface deflection is then used to make up for the lack of asymmetric thrust available, as shown in Figs. 5b and 5c. This result was expected and desired, showing that the engine yaw add-on met the commanded yaw moment when possible, but would always track the total thrust command, as seen in Fig. 5d.

Robustness of the control law was evaluated in simulation in order to determine modifications that may be necessary prior to implementation on a flight vehicle. The robustness was evaluated with respect to aerodynamic model errors and noise in the engine rpm sensor. Aerodynamic modeling errors were tested with a 50-percent increase and decrease from nominal for the split-aileron control effectiveness. Results for a rudder step are shown in Figs. 6a through 6c. Overestimating the aerodynamic effectiveness (+50% model error) improves the response time of the engine yaw add-on while underestimating the control effectiveness (-50% model error) degrades the response time, as shown in Fig. 6a. Convergence time with a +50% model error is approximately 10 s faster than nominal and the time with -50% model error is approximately 30 s longer than nominal. This result is due to the control effectiveness errors acting as a gain on the yaw moment portion of the cost function in Eq. (1); effectively weighting the yaw moment objective higher or lower than the nominal case. The same steady-state is reached with both the nominal and aerodynamic error simulation runs, Figs. 6b and 6c, showing that the engine yaw add-on is robust to aerodynamic modeling errors of this magnitude.

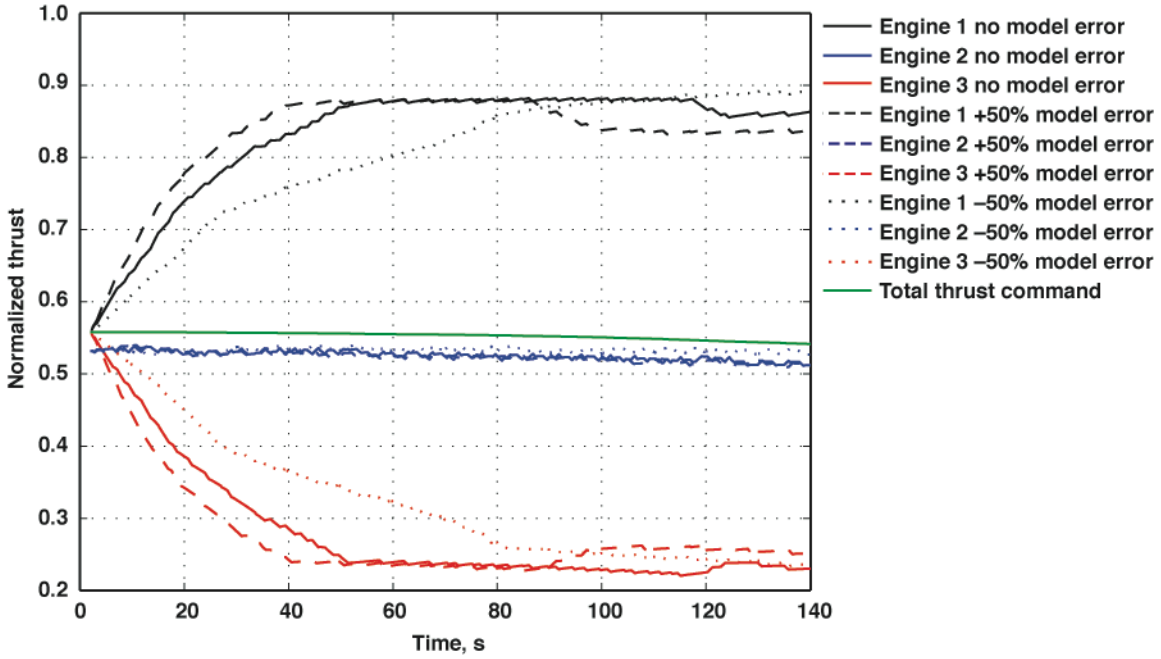

Figure 6a. Individual thrust response, rudder step aero model error.

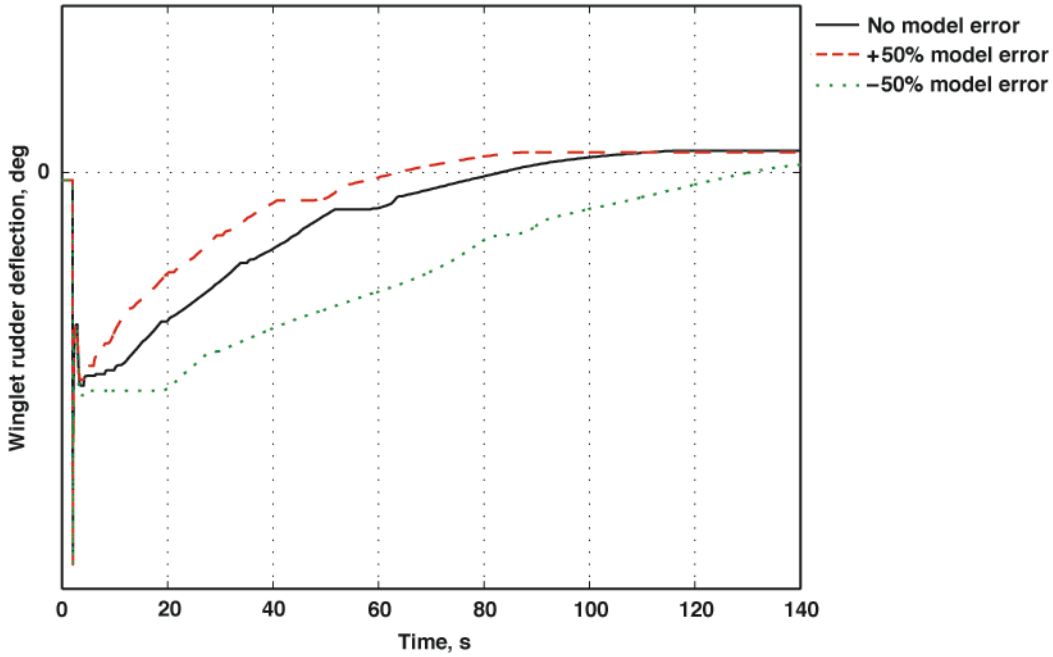

Figure 6b. Winglet rudder response, rudder step aero model error.

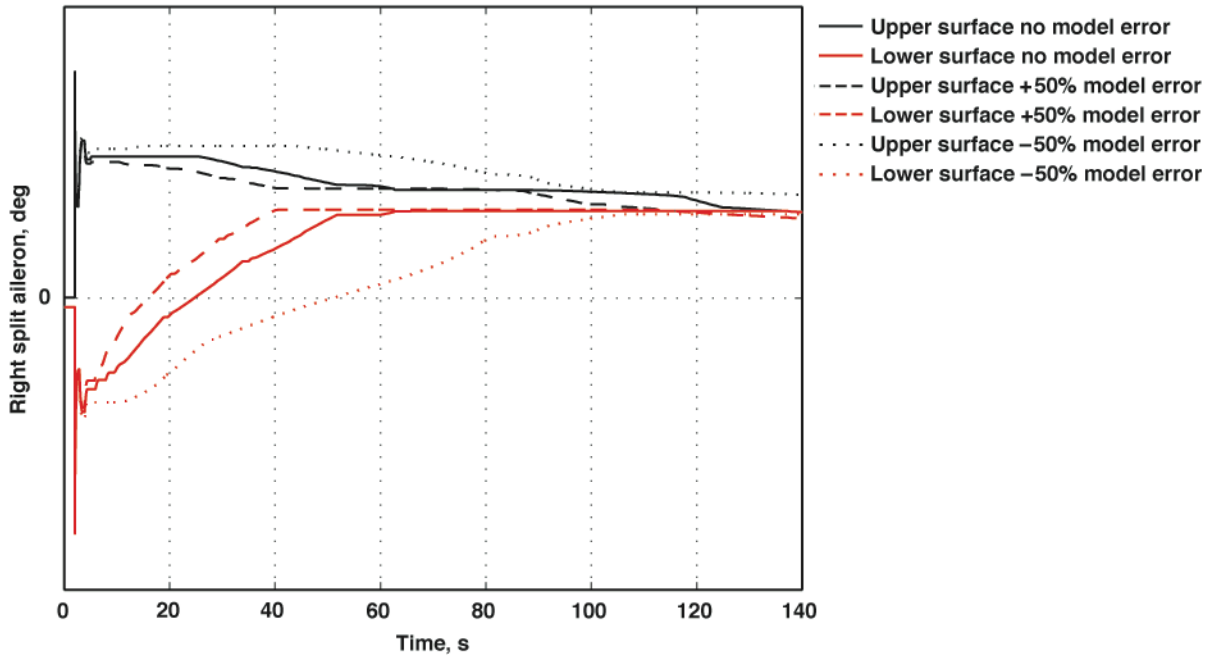

Figure 6c. Right split aileron response, rudder step aero model error.

Effects of noise in the measured rpm during a rudder step maneuver are shown in Figs. 7a through 7c. Random noise equal to 5% of the maximum rpm was added to the measured signal, which is well above the expected noise in flight. Engine commands were noisy, as shown in Fig. 7a, and convergence time was lengthened from approximately 50 s to approximately 70 s, as seen in Figs. 7a and 7c. Winglet rudder deflection, however, was reduced, as shown in Fig. 7b, and the split ailerons were driven close to zero, as shown in Fig. 7c, so the engine yaw control appears to be robust to this level of measurement noise.

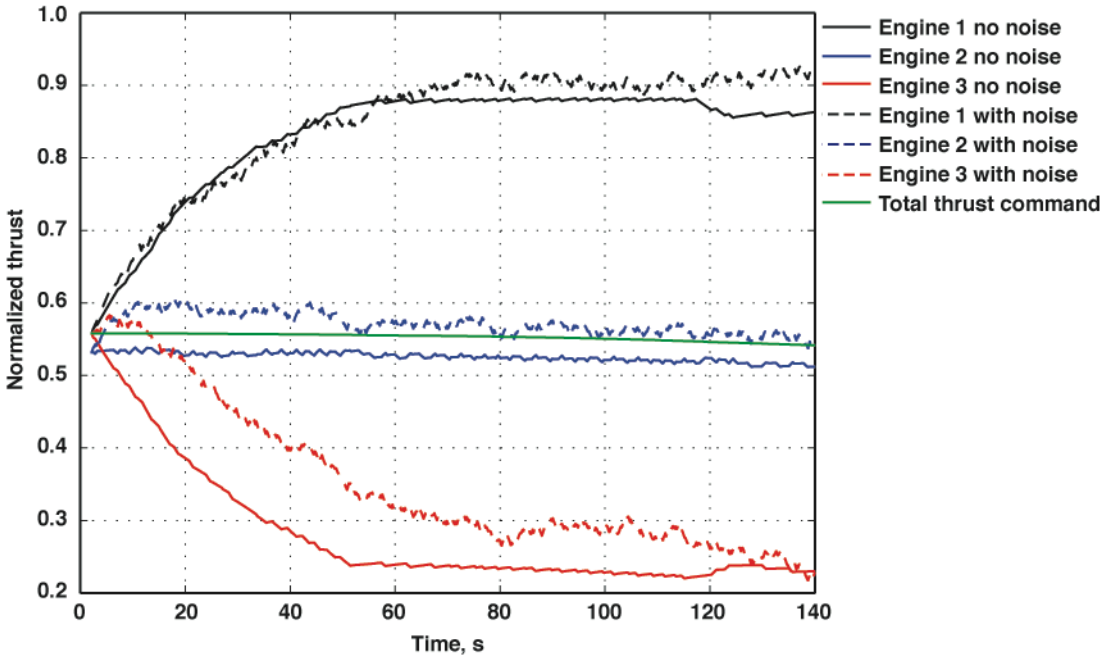

Figure 7a. Individual thrust response, rudder step rpm noise.

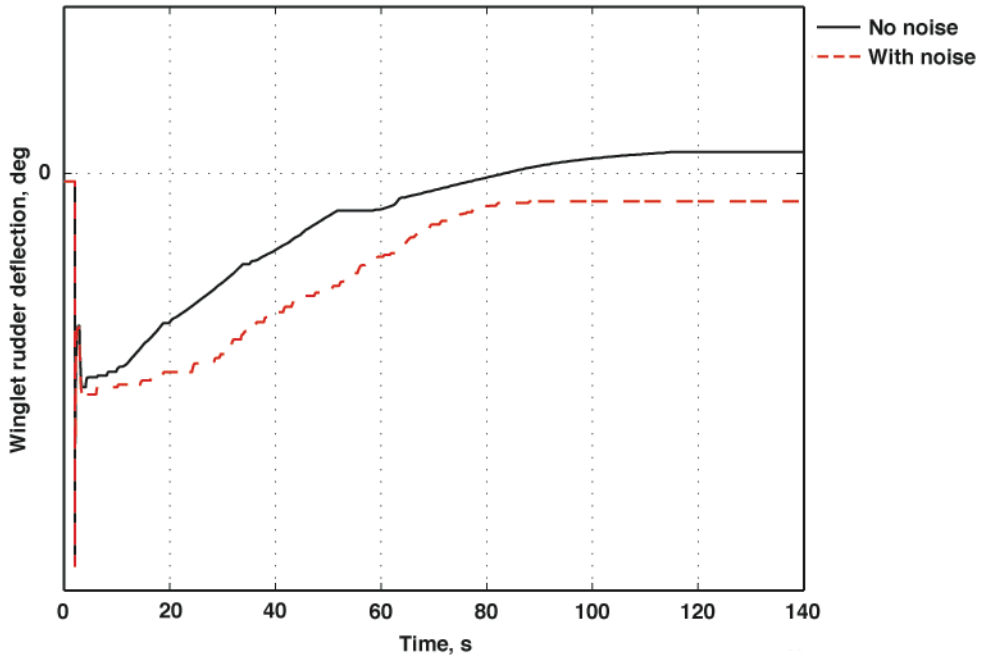

Figure 7b. Winglet rudder response, rudder step rpm noise.

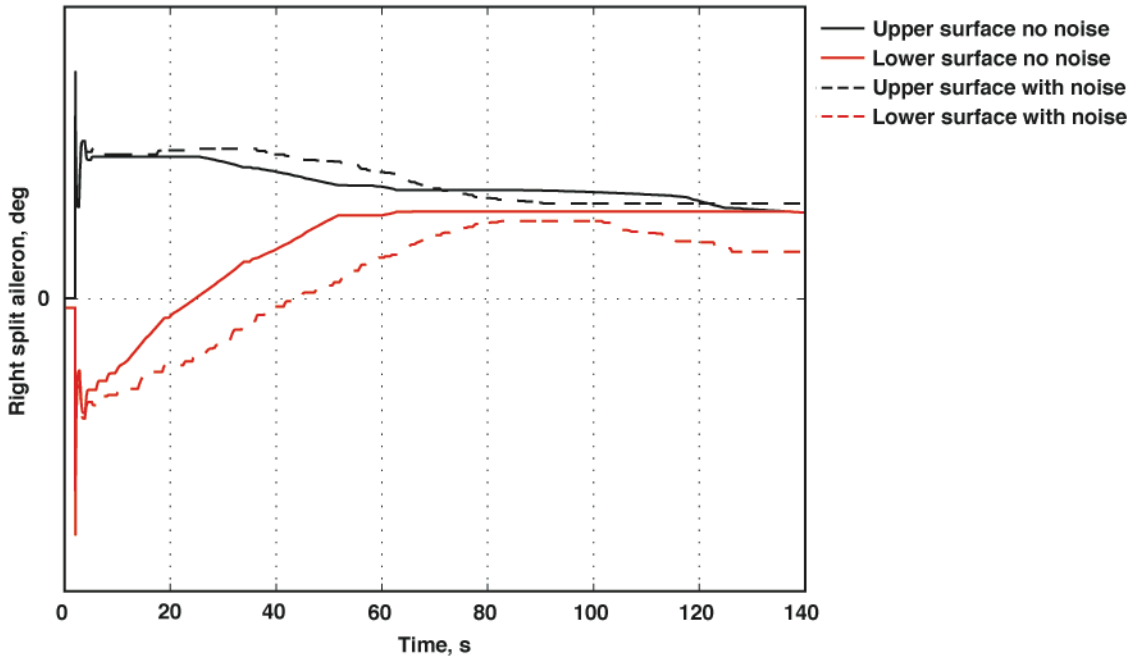

Figure 7c. Split aileron response, rudder step rpm noise.

Occurrences of split-aileron deflection during level, zero-sideslip flight have been observed during X-48B flight-testing, as shown in Fig. 8. For the X-48B, the engine yaw add-on has the potential to reduce drag by 2 to 4 percent, depending on flight condition. This estimation is based on the maximum yaw generation capability of the engine yaw add-on and the amount of drag the split ailerons would need to create the same yaw moment. For the specific case shown in Fig. 8, it is estimated that the split ailerons could be fully driven to zero by the engine yaw add-on at this flight condition and drag would be reduced by approximately 2.8 percent.

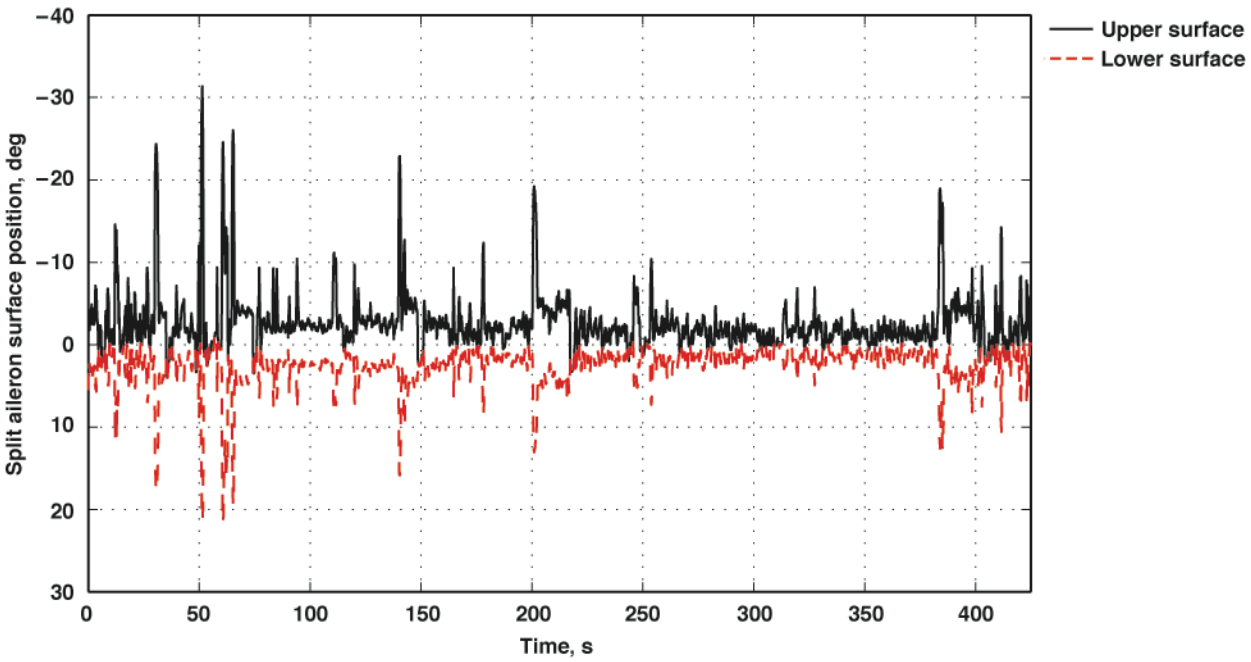

Figure 8. The X-48B split aileron deflection in flight.

V. Conclusion

Asymmetric engine thrust was used to reduce deployment of aerodynamic surfaces for yaw control on the X-48B aircraft (The Boeing Company, Chicago, Illinois) and was tested in non-linear simulation. Designed as an add-on to the baseline control laws, the goals were to preserve the baseline aircraft control characteristics and to reduce drag. These goals were accomplished with the use of optimal control allocation techniques that tracked the total thrust command, generated yaw moment in order to drive the aerodynamic yaw surfaces to zero, and kept the individual engines as close to their individual power level angle commands as possible. Testing in simulation demonstrated that the engine yaw add-on did not degrade the baseline lateral-directional stability and control of the aircraft. Thrust tracking and driving aerodynamic surfaces to zero was demonstrated under nominal conditions as well as with aerodynamic modeling errors and sensor noise. This add-on control law has the potential to reduce drag 2 to 4 percent for the X-48B aircraft. The technology presented in this paper could be applied on future hybrid-wing-body aircraft to enhance their fuel efficiency and help meet Environmentally Responsible Aviation and national goals. Planned future research includes flight-testing the engine yaw control on the X-48C aircraft to demonstrate its feasibility in a flight environment.

References

[1]Collier, F., "Overview of NASA's Environmentally Responsible Aviation (ERA) Project," 48th AIAA Aerospace Sciences Meeting, Orlando, Florida, January, 2010.

[2]Risch, T. K., "Blended Wing-Body (BWB) Low Speed Vehicle X-48B Blocks 1 and 2 Flight Data Report," NASA TM-2010-214653/VOL1, April 2010 (available from the X-48B project manager, Dryden Flight Research Center, Edwards, California).

[3]National Transportation Safety Board, Aircraft Accident Report, "United Airlines Flight 232, McDonnell Douglas DC-10-10, Sioux Gateway Airport, Sioux City, Iowa, July 19, 1989," PB90-910406, NTSB/ARR-90/06.

[4]Burcham, F. W. Jr., Burken, J., and Maine, T., "Flight Testing a Propulsion-Controlled Aircraft Emergency Flight Control System on an F-15 Airplane," AIAA-1994-2123-CP, 1994.

[5]Burken, J. J., and Burcham, F. W. Jr., "Flight-Test Results of Propulsion-Only Emergency Control System on MD-11 Airplane," *Journal of Guidance, Control, and Dynamics*, Vol. 20, No. 5, 1997, pp. 980-987.

[6]Burken, J. J., Burcham. F. W. Jr., Maine, T. A., Feather, J., Goldthorpe, S., and Kahler, J. A., "Flight Test Of A Propulsion-Based Emergency Control System on the MD-11 Airplane with Emphasis on the Lateral Axis," NASA-TM-4746, 1996.

[7]Jonckheere, E. A., Yu, G.-R., and Chien, C.-C., "Gain Scheduling for Lateral Motion of Propulsion Controlled Aircraft Using Neural Networks," *Proceedings of the American Control Conference*, 1997, pp. 3321-3325.

[8]Jonckheere, E. A., and Yu, G.-R., "Propulsion Control of Crippled Aircraft by H_∞ Model Matching," *IEEE Transactions On Control Systems Technology*, Vol. 7, No. 2, 1999, pp. 142-159.

[9]Liu, Y., Tang, X., and Tao, G., "Adaptive Failure Compensation for Aircraft Flight Control Using Engine Differentials: Regulation," AIAA-2005-6996, 2005.

[10]Liu, Y., Tang, X., Tao, G., and Joshi, S. M., "Adaptive Compensation of Aircraft Actuation Failures Using an Engine Differential Model," *IEEE Transactions On Control Systems Technology*, Vol. 16, No. 5, 2008, pp. 971-982.

[11]Yu, G.-R., and Chen S.-H., "Explicit Model-Following Design of Integrated Flight and Propulsion Control Systems," *Proceedings of 2005 CACS Automatic Control Conference*, 2005.

[12]Stepanyan, V., Krishnakumar, K., and Nguyen, N., "Adaptive Control Of a Transport Aircraft using Differential Thrust," AIAA-2009-5741, 2009.

[13]Kaneshige, J., and Gundy-Burlet, K., "Integrated Neural Flight and Propulsion Control System," AIAA-2001-4386, 2001.

[14]Gundy-Burlet K., Krishnakumar, K., Limes, G., and Bryant, D., "Augmentation of an Intelligent Flight Control System for a Simulated C-17 Aircraft," *Journal of Aerospace Computing, Information, and Communication*, Vol. 1, 2004, pp. 526-542.

[15]Urnes, J. M., and Nielsen, Z. A., "Use of Propulsion Commands to Control Directional Stability of a Damaged Transport Aircraft," AIAA-2010-3470, 2010.

[16]Duke, B., Hathaway, R., and Pineiro, L., "Extended Range Demonstration on the F-15 ACTIVE," World Aviation Congress, Sept. 1998.

[17]Risch, T., Cosentino, G., Regan, C. D., Kisska, M., and Princen, N., "X-48B Flight-Test Progress Overview," AIAA-2009-934, 2009.

[18]Harkegard, O., "Backstepping and Control Allocation with Applications to Flight Control," *Linkoping Studies in Science and Technology*, Dissertation No. 820, Linkoping, Sweden, 2003.